Proceedings of the ASME 2018
Dynamic Systems and Control Conference
DSCC2018
September 30-October 3, 2018, Atlanta, Georgia, USA

DSCC2018-8969

THE EFFECT OF NONLINEAR SPRINGS IN JUMPING MECHANISMS

Sahand Sadeghi*, Blake D. Betsill, Phanindra Tallapragada, and Suyi Li
Department of Mechanical Engineering
Clemson University
Clemson, SC, USA

ABSTRACT

This research investigates the potential effects of utilizing nonlinear springs on the performance of robotic jumping mechanisms. As a theoretical example, we study dynamic characteristics of a jumping mechanism consisting of two masses connected by a generic nonlinear spring, which is characterized by a piecewise linear function. The goal of this study is to understand how the nonlinearity in spring stiffness can impact the jumping performance. To this end, non-dimensional equations of motion of the jumping mechanism are derived and then used extensively for both analytical and numerical investigations. The nonlinear force-displacement curve of the spring is divided into two sections: compression and tension. We examine the influences of these two sections of spring stiffness on the overall performance of the jumping mechanism. It is found that compression section of the nonlinear spring can significantly increase energy storage and thus enhance the jumping capabilities dramatically. We also found that the tension section of the nonlinear force-displacement curve does not affect the jumping performance of the center of gravity, however, it has a significant impact on the internal oscillations of the mechanism. Results of this study can unfold the underlying principles of harnessing nonlinear springs in jumping mechanisms and may lead to the emergence of more efficient hopping and jumping systems and robots in the future.

1. INTRODUCTION

Studying legged robots is a century-old branch of robotic studies [1]. The aspiration of replicating the omnipresent legged animals that are able to overcome the unfavorable environmental conditions have engaged more and more robotic researchers in this field [2,3]. However, the dynamics of legged robots are quite complicated compared to the stationary and wheeled mobile robots, especially due to the impact with the ground. This, along with several other issues such as complex nonlinear control, has led researchers to focus on single-legged systems that possess a much simpler configuration [4]. The locomotion of single-legged robotic systems is achieved by hopping. Hopping is the process of utilizing stored energy of the system to jump and it can occur repeatedly via storing and then reusing the energy during landing [5]. Despite its relative simplicity, hopping is still a useful means of locomotion especially in terrains that are inaccessible to wheeled or tracked systems [4]. It can also be very advantageous in situations when there is a sudden need for reflex, e.g. frogs or bush-babies take advantage of their innate hopping ability to flee from predators. Recently, there have been plenty of valuable researches on different aspects of jumping locomotion, from proposing novel hopping mechanisms [6–9] to various control strategies for stabilizing the dynamic motion [10–13].

One can discern three pivotal topics of research among the recent investigations on hopping or jumping robots: Actuators, energy storage, and dynamics of hopping. Actuator has always been one of the main concerns of researches in this field. Since the very first hopping mechanism prototype proposed by Matsuoka [14], researchers have been seeking more efficient actuators that can provide a low-cost, lightweight and safe actuation. Several prominent researches in the field of hopping robots have been inspired by the mechanism designed by Raibert [15,16], which utilizes hydraulic and pneumatic actuators. Other works utilized electric actuators that are cleaner, safer, less expensive, and more appropriate for autonomous robots [4,7,17]. Besides actuators, energy storage also plays a significant role in the performance of hopping robots. All of the existing jumping mechanisms rely on the instant release of the stored energy to realize jumping [7], and there are several approaches to achieve the required energy storage . Implementing traditional springs, such as compression, extension, or torsion springs, is probably the most popular method [7,18–21]. Compressed air is another method of energy storage [7] that has been used in rescue [22] and patrol

* Corresponding author: ssadegh@clemson.edu

robots [23]. Several researchers have also implemented specialized elastic elements or customized springs [7] for storing energy. For example, the MIT microbot utilizes two symmetrical carbon fiber strips with dielectric elastomer actuators [24,25], Jollbot deforms its spherical shape to store energy [26], and another compact jumping robot takes advantage of an elastic strip to form closed elastica actuated by two revolute joints [27,28].

The dynamics of hopping robots is another important branch of robotic research for deciphering the underlying principles of hopping. Hopping mechanisms exhibit a nonlinear dynamic behavior, naturally. This is especially due to the impact with the ground and the presence of distinct stance and flight phases with sudden transitions [4]. The governing dynamics of these two main phases are fundamentally different. Researchers have conducted several studies on the nonlinear dynamics of hopping. For example, M'Closkey and Burdick investigated forward running dynamics of a 2-DOF hopper using a Poincare' return map [29]. Koditschek and Buehler modified the Raibert's model and studied two discrete dynamical models of this vertical hopper using linear and nonlinear spring [10]. The nonlinear springs can introduce unique and desirable dynamic characteristics to the hopping mechanisms. They were utilized in several jumping prototypes and their effects on the overall dynamic performances were assessed. For example, Yamada et al. proposed the idea of using snap-through buckling – an archetypical nonlinear stiffness property – of a closed elastica for jumping robots [27,28]. In another study, Fiorini and Burdick implemented a linear spring in a 6-bar geared mechanism to generate an effective nonlinear spring behavior and investigated its effects on overcoming the pre-mature take-off [30]. In addition, through a preliminary study, Armour investigated the effect of negative stiffness on jumping [26]. However, apart from these experimental case studies, there is a lack of any comprehensive analysis on the potential benefits of utilizing nonlinear springs to improve the performance of the hopping and jumping mechanisms. Such a gap in our knowledge prevents us from building hopping robots that can effectively exploit nonlinear springs. Therefore, the aim of this research is to fill this void by analyzing the performance of a generic jumping mechanism consisting of two identical masses connected by a nonlinear spring. To this end, we use a piecewise linear function, as an archetype example, to characterize the force-displacement relationship of the nonlinear springs. The outcome of this research can provide guidelines for robotic researchers and foster more efficient hopping mechanisms and robots in the future.

The rest of this paper is organized as follows. In section 2, we introduce the generic jumping mechanism utilizing a nonlinear spring as the energy storage element. Then we derive the non-dimensional equations of motions that govern the jumping phenomenon. In section 3, we analyze the potential merits of utilizing a nonlinear spring element through an extensive study based on numerical simulations and analytical reasoning. Finally, section 4 concludes the paper with a summary and discussion.

2. JUMPING MECHANISM AND ITS EQUATIONS OF MOTION

The jumping mechanism (figure 1) investigated consists of two identical masses connected by an elastic element exhibiting non-linear stiffness characteristics. Energy storage in the system occurs through exerting an input force using an actuator on the top mass to deform the elastic element. The reaction force-displacement relationship of the nonlinear spring can be generally represented by a C^n $(n \geq 0)$ continuous curve. However, in order to avoid introducing unnecessary complexities, we focus on a generic piecewise linear C^0 curve to describe the nonlinear stiffness properties. Despite its relative simplicity, the C^0 curve is a useful tool for approximating many nonlinear stiffness properties commonly used for engineering applications, e.g. negative stiffness [31] and quasi-zero stiffness [32,33] characteristics. Figure 2(a) shows the C^0 piecewise linear force-displacement curve that will be used in this study. The displacement axis is represented by y, where $y = Y_2 - Y_1 - l_0$. Y_1 and Y_2 are the height of the two masses with respect to the ground, and l_0 is the free length of the nonlinear spring. This curve consists of four linear sections with different stiffness coefficients (K_1 to K_4). We also consider the structural and actuation limit that can constrain the problem. The structural limit (H) is the maximum relative displacement between the two masses in order to compress the spring and store an initial energy. The actuation limit is the maximum amount of external force (f_c) the actuator can provide. Moreover, the force-displacement curve can be divided in to two separate regions: The compression region (negative displacement), where the spring is compressed; and the tension region (positive displacement), where the spring is under tension. This separation allows us to study the energy storage (compression) and jumping dynamics (tension) in a more systematic approach, as we will see later in section 3.

Knowing the reaction force of the nonlinear spring, we can now investigate the dynamic behavior of the system. The dynamic motion of the jumping mechanism can be divided into two

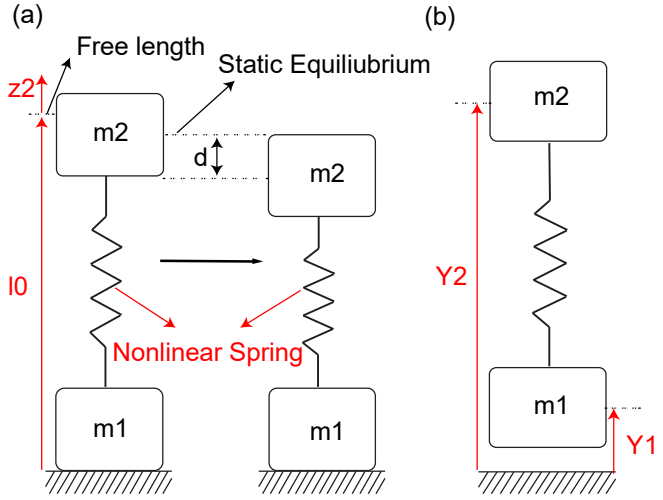

Figure 1. Schematic of the jumping mechanism in (a) pre-jump phase of motion and (b) post-jump phase of motion.

different phases: 1) pre-jump phase and 2) post-jump phase. In order to just focus on the potential effects of the nonlinear spring, we assumed that the masses are equal: $m_1 = m_2 = m$. In the following two sections, we study the motion of the system in these two phases.

2.1. PRE-JUMP PHASE OF MOTION

The pre-jump phase (figure 1(a)) occurs for all time prior to the bottom mass m_1 leaving the ground. During this phase, an input actuation force displaces m_2 up to a certain initial position (d). Once the input force is removed, the reaction force of the spring accelerates the upper mass upward. The governing equation of motion during this phase can be represented by:

$$m\ddot{Y}_2 = -F(Y_2 - l_0) - mg, \tag{1}$$

where m is the mass of the upper body, $F(Y_2 - l_0)$ is the reaction force of the spring, and $\ddot{Y}_2$ and Y_2 represent the acceleration and position of the upper mass (relative to the ground), respectively. We define $k^* = f_c / H$, the ratio between actuation limit and structural limit, as a reference linear spring coefficient. Equation (1) can be non-dimensionalized as follows:

$$\frac{d^2\hat{Y}_2}{d\tau^2} + \hat{F}(\hat{Y}_2 - \hat{l}_0) = -\hat{G}, \tag{2}$$

where, $\hat{Y}_1 = \frac{Y_1}{H}$, $\tau = t\omega$, $\omega = \sqrt{\frac{k^*}{m}}$, $\hat{F} = \frac{F}{f_c}$, $\hat{l}_0 = \frac{l_0}{H}$ and $\hat{G} = \frac{mg}{f_c}$. We can also non-dimensionalize the stiffness coefficients: $\hat{k}_i = \frac{k_i}{k^*}$, $(i = 1, 2, ..., 4)$.

2.2. POST-JUMP PHASE OF MOTION

In order for a jump to be possible, the jumping mechanism must be capable of surpassing the gravitational force once the displacement in the non-linear elastic element has become positive. That is, the restoring force of the non-linear elastic element acting on the lower mass must exceed its weight. The jumping occurs when $\hat{Y}_2 = \hat{Y}_{2,jump}$, where:

$$\hat{F}(\hat{Y}_{2,jump} - \hat{l}_0) = \hat{G}. \tag{3}$$

The airborne or post-jump phase of the motion is illustrated in figure 1(b). Once the bottom mass has left the ground, the governing system of coupled equations of motion can be defined as:

$$\begin{aligned} m\ddot{Y}_1 &= F(Y_2 - Y_1 - l_0) - mg, \\ m\ddot{Y}_2 &= -F(Y_2 - Y_1 - l_0) - mg. \end{aligned} \tag{4}$$

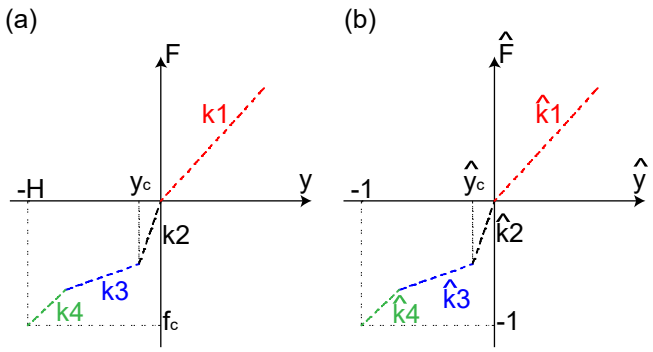

Figure 2. (a) Piecewise linear reaction force-displacement curve of spring with structural and actuation limits. (b) Non-dimensional force-displacement curve.

Following the same procedure of section 2.1, we can derive the non-dimensional system of equations as follows:

$$\begin{aligned} \frac{d^2\hat{Y}_1}{d\tau^2} &= F(\hat{Y}_2 - \hat{Y}_1 - \hat{l}_0) - \hat{G}, \\ \frac{d^2\hat{Y}_2}{d\tau^2} &= -F(\hat{Y}_2 - \hat{Y}_1 - \hat{l}_0) - \hat{G}. \end{aligned} \tag{5}$$

The initial conditions of equation 5 can be extracted from the solution of pre-jump phase (equation 2). In the next section, we present the numerical simulation results of solving the equations of motion.

3. STUDYING THE EFFECT OF FORCE-DISPLACEMENT PROFILE OF THE NONLINEAR SPRING ON THE JUMPING PERFORMANCE

Jumping occurs when the upper mass in figure 1 reaches a specific height (equation 3), as we mentioned earlier. At this point, the lower mass loses its contact with the ground and jumps off the ground. At the transition stage when the jump starts, most of the stored energy in the spring (E_0) is converted to the kinetic energy of the upper mass and some portion will be converted to gravitational potential energy. We assume that the whole mechanism is subject to conservative forces and no damping is involved. Therefore, during the post jump phase when both of the masses are airborne, the total energy of the system (aka. kinetic energy + spring potential energy + gravitational potential energy) will be conserved. Nevertheless, we expect that two different masses of the mechanism exhibit complex behaviors after jumping due to the presence of a nonlinear spring element. Therefore, it is important to study both the responses of the masses individually and the movement of the overall center of gravity in order to obtain a clear understanding of the dynamic behaviors. To this end, we start our investigation by analyzing the effect of the stored energy on the jumping performance. The stored energy is related to the compression (negative displacement) section of the force-displacement curve. Therefore, the first objective would be to gain an accurate comprehension of the underlying principles

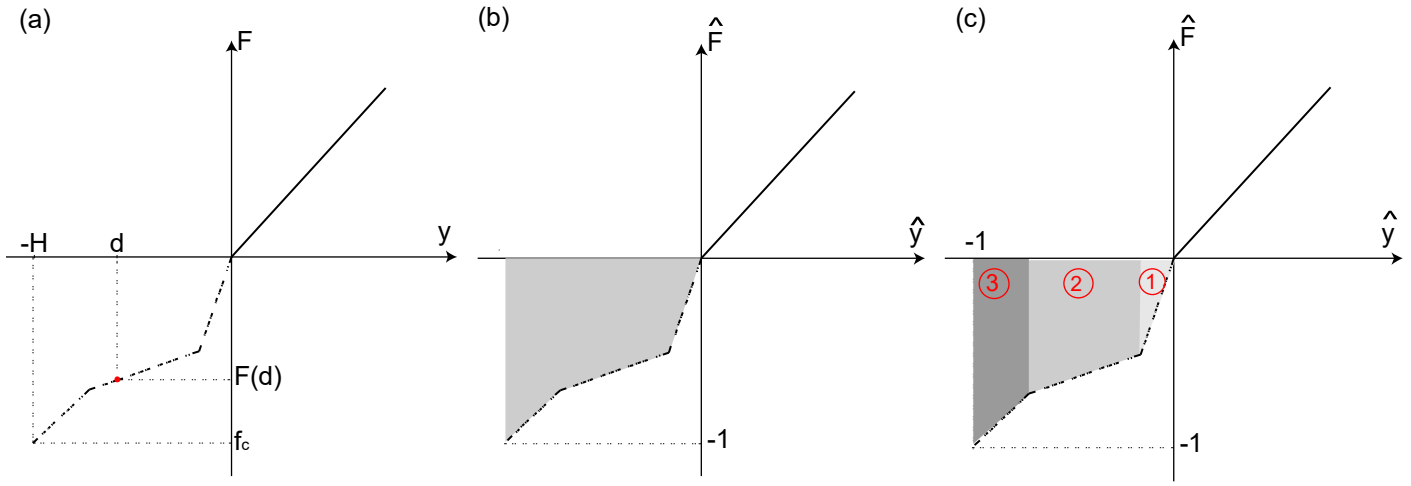

Figure 3. (a) Reaction force-displacement curve of the spring with an initial displacement (d). (b) Non-dimensional force-displacement curve of the spring with the shaded area representing the initial stored energy. (c) Three constituent areas of the shaded region.

that regulate the relation between the compression section of the force-displacement curve and the jumping phenomenon (section 3.1). In order to acquire a comprehensive tool for designing a jumper with a desired functionality, we also investigate the effect of the tension (positive displacement) section of the force-displacement curve on the jumping behavior of the overall center of gravity and both masses (section 3.2).

3.1. ENERGY STORAGE AND THE COMPRESSION (NEGATIVE DISPLACEMENT) SECTION OF THE FORCE-DISPLACEMENT CURVE

Storing energy in the system, shown in figure 1, is achieved by compressing the spring element to an initial displacement. The stored energy (E_0) at this stage is equal to the amount of work (W_{ext}) that has been done on the spring to compress it. The relationship between the stored energy and the restoring force of the spring, if it is compressed from the free length, can be expressed as:

$$E_0 = W_{ext} = \int_0^d F(y).dy, \tag{6}$$

where d is the displacement of the spring from the free length and $F(y)$ represents the restoring force of the spring (figure 3(a)). As we mentioned in section 2, a piecewise linear force-displacement curve (figure 2) is an advantageous tool for representing most of the nonlinear stiffness properties that have been used for engineering applications. Therefore, in this section we focus on the generic piecewise linear force-displacement curves constrained by the actuation and structural limits (figure 2(b)) to study the effect of nonlinear spring elements on the jumping phenomenon.

To obtain a better insight into the energy storage function, we first non-dimensionalize equation 6 based on the structural and actuation limit so that,

$$\hat{E}_0 = \int_0^{\hat{d}} \hat{F}(\hat{y}).d\hat{y}, \tag{7}$$

where:

$$\hat{E}_0 = \frac{E_0}{\frac{1}{2}k^* H^2},\ \hat{d} = \frac{d}{H}.$$

Two important factors affect the amount of stored energy in the mechanism, namely initial displacement and the force-displacement function. It is clear that for a given force-displacement relationship, one can store the maximum amount of energy when the mechanism is initially compressed all the way up to its structural limit, that is $\hat{d} = -1$.

Meanwhile, shape of the force-displacement curve plays a significant role as well. Consider an arbitrary piece-wise linear curve in the negative displacement region, bounded by the two structural and actuation limits ($\hat{d} = -1$ and $\hat{F}(d) = -1$, figure 3b). The stored energy of the system is equal to the area between the $\hat{y}$ - axis and the $\hat{F}(\hat{y})$ curve (shaded region in figure 3(b)). The area can be represented by the summation of three constituent areas, one triangle (A_1) and two trapezoids (A_2 and A_3) (figure 3(c)), as follows:

$$\hat{E}_0 = A_1 + A_2 + A_3 \tag{8}$$

The compression section of the generic force-displacement curve consists of three piecewise linear curves with three different non-dimensional stiffness coefficients: $\hat{k}_2$, $\hat{k}_3$ and $\hat{k}_4$. The magnitudes of these three stiffness coefficients can be varied to examine the effect of energy storage on the jumping behavior. Figure 4(a) demonstrates three different piecewise linear force-

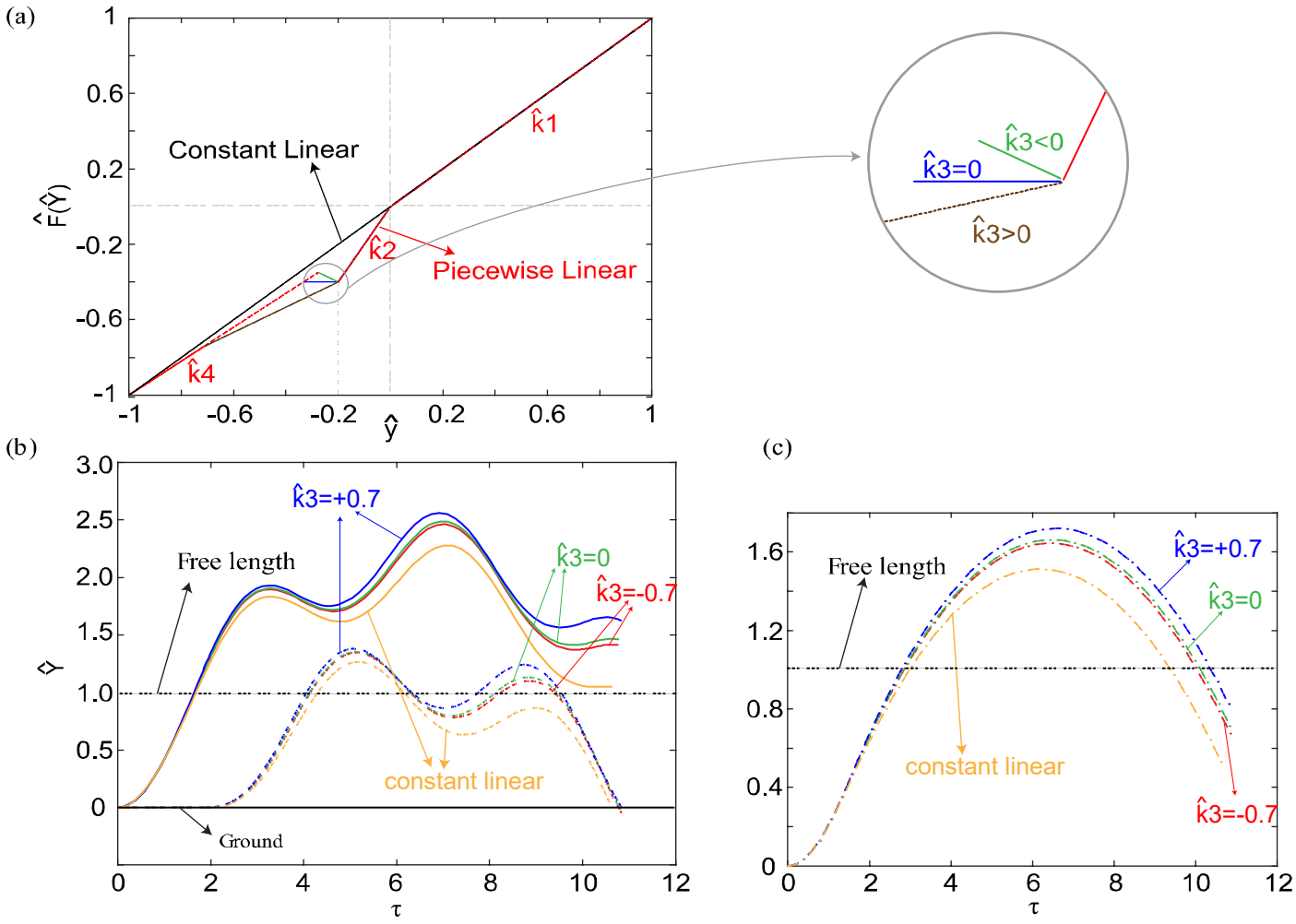

Figure 4. (a) Three different piecewise linear force-displacement curves, with positive, negative and zero $\hat{k}_3$ stiffness coefficients. (b) Vertical displacement of the upper mass (solid line) and lower mass (dashed line). (c) Vertical displacement of the center of gravity.

displacement curves with a positive, negative, and zero $\hat{k}_3$ coefficient, respectively. Another "constant linear" force-displacement curve with stiffness coefficient $\hat{k}=1$ is also plotted in this figure for reference. Constant linear force-displacement curve is a linear curve with a constant stiffness throughout its domain. Indeed, this constant linear force-displacement relationship can lead to the largest possible stored energy among all of the linear stiffness curves bounded by the structural and actuation limit. Therefore, it represents the best possible linear spring. We assume the three piecewise linear curves share the same $\hat{k}_1$, $\hat{k}_2$ and $\hat{k}_4$ stiffness coefficients and $\hat{y}_c$. In addition, we choose the tension stiffness of all three piecewise linear springs to be the same as the fully linear spring, that is $\hat{k}_1=\hat{k}=1$, in order to compare the performance of nonlinear and linear springs. All of the piecewise linear curves are chosen to provide more stored energy than the constant linear spring.

We used MATLAB ODE45 solver to solve the system of ordinary differential equations governing the motion, presented by equation 2. Initial condition of the upper mass is chosen as [$\hat{Y}_2=0, \hat{\dot{Y}}_2=0$] where $\hat{Y}_2$ is measured from the ground. Additionally, Initial conditions of the post-jump phase of motion presented by equation 5, is extracted from the solution of pre-jump phase (governed by equation 2).

Figure 4(b) and 4(c) show the vertical displacement of both masses and the center of gravity. Based on the results, it can be seen that the jumping mechanisms featuring piecewise linear springs outperform the one with constant linear springs in terms of jumping distances (up to 14% increase). Furthermore, both of the masses and also the center of gravity are able to reach higher heights when $\hat{k}_3$ is positive. This is because the mechanisms with positive $\hat{k}_3$ stiffness coefficients are able to store more energy due to the larger area between the displacement axis and the force-displacement curve (aka. larger A_2 in figure 3). Besides jumping height, we also compare the energy efficiency of these mechanisms. The ability of reaching higher heights in piecewise linear springs stems from their capability of storing

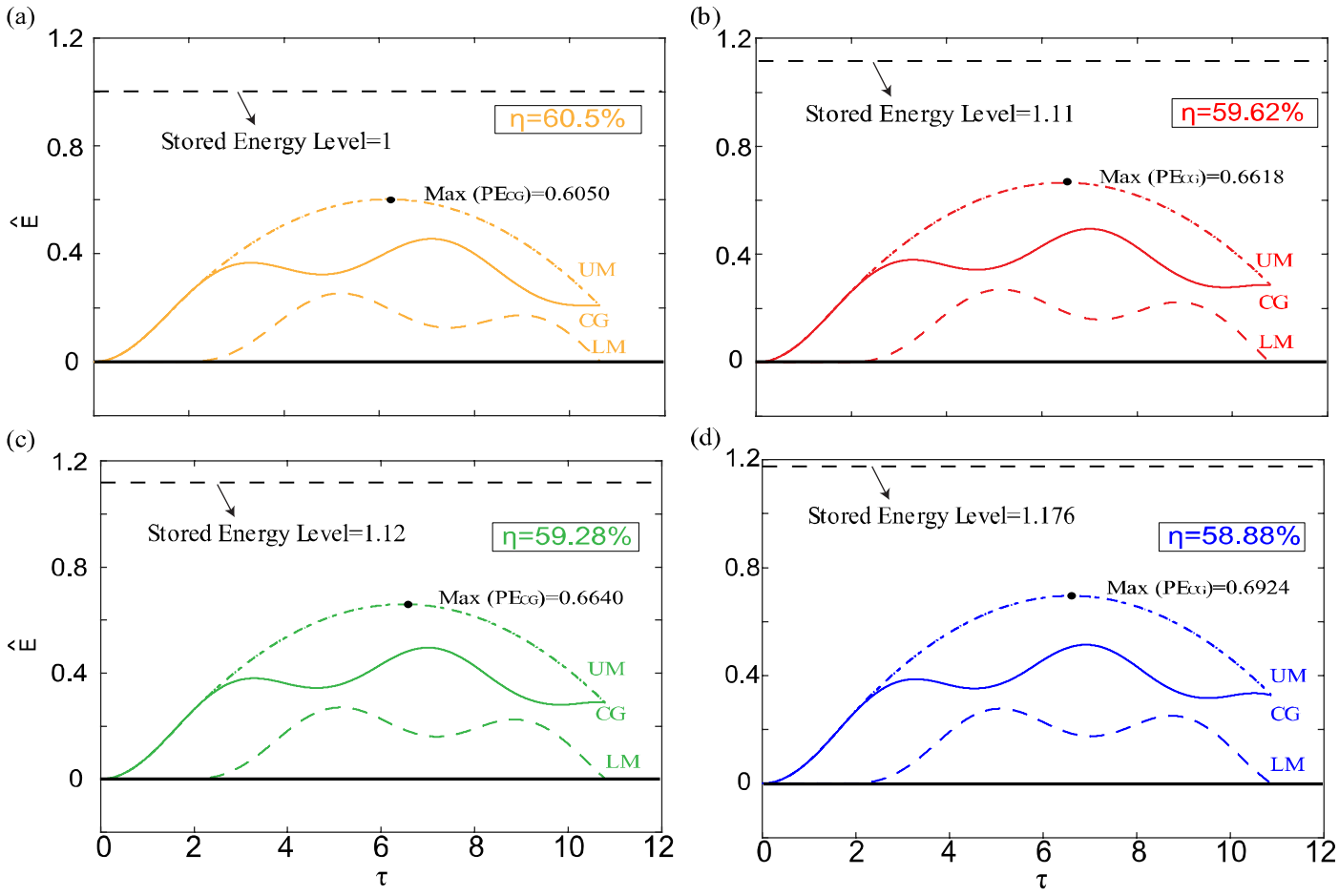

Figure 5. (a) Gravitational potential energy levels of the upper mass (UM), lower mass (LM) and center of gravity (CG) for constant linear stiffness (a); and three piecewise linear cases (b-d). The three piecewise linear force-displacement curves feature the same $\hat{k}_1 = 1$, $\hat{k}_2 = 2$, $\hat{k}_4 = 0.9$, $\hat{y}_c = -0.2$. But they have different $\hat{k}_3$ values: (b) $\hat{k}_3 = -0.7$, (c) $\hat{k}_3 = 0$ and (d) $\hat{k}_3 = +0.7$.

more energy in the system. Therefore, it is important to analyze the efficiency of utilizing this additional energy. We define the energy efficiency of the mechanism as the ratio between the maximum gravitational potential energy of the overall center of gravity ($\max(PE_{CG})$) and the initial stored energy (E_0):

$$\eta = \frac{\max(PE_{CG})}{E_0} \times 100 \tag{9}$$

Figure 5(a-d) shows the gravitational potential energies of three different systems presented in figure 4. Also shown in this figure is the initial stored energy level. Based on these results, we can observe that the mechanism utilizing the piecewise linear spring exhibit a slight drop in energy efficiency (<2% for the spring with positive $\hat{k}_3$).

We further analytically investigate this efficiency drop for the mechanisms with higher initial stored energy. Consider the initial stored energy of a mechanism utilizing a constant linear spring with stiffness coefficient $\hat{k} = 1$. We can represent the non-dimensional initial stored energy of the system by $\hat{E}_0$, where:

$$\hat{E}_0 = \frac{E_0}{E_{0,linear\ spring}} = \frac{E_0}{\frac{1}{2}k^* H^2} = 1 + \hat{e}, \tag{10}$$

where $\hat{e}$ ($0 \le \hat{e} \le 1$) represents the additional non-dimensional stored energy by utilizing a nonlinear properties in the compression section of the force-displacement curve. One can represent the difference between the efficiencies of the nonlinear system and the linear system by the following equation:

$$\Delta\eta = \eta_{linear} - \eta_{non-linear} = \left(\frac{\max(PE_{CG,linear})}{\hat{E}_{0,linear}} - \frac{\max(PE_{CG,nonlinear})}{\hat{E}_{0,linear} + \hat{e}} \right) \times 100. \tag{11}$$

By considering the fact that the additional energy due to utilizing a nonlinear spring will be converted to the kinetic energy of the system at the free length and with some mathematical work, one can show that:

$$\eta_{linear} - \eta_{non-linear} = \left(2\hat{G}\frac{\hat{e}}{1+\hat{e}} \right) \times 100. \quad (12)$$

This equations implies that the efficiency drop of a nonlinear mechanism follows a hyperbolic relationship with respect to the additional energy $\hat{e}$. If more energy is stored in the pre-jump phase via using nonlinear springs, jumper mechanism becomes less efficient. However, it is important to point out that this drop in efficiency is linearly dependent on $\hat{G}$, which is the ratio of the jumping mechanism mass over the maximum spring reaction force (aka. actuation limit). For a typical jumping mechanism, this ratio is designed to be small and significantly less than one. In our case study, $\hat{G} = 0.1$. As a result, the magnitude of the efficiency drop from using nonlinear spring is small (less than 2% in our case studies). The benefit of significantly higher jump distance (up to 14% increase) easily outweigh the small sacrifice in terms of efficiency.

Therefore, our results elucidate that implementing nonlinear spring can significantly increase the jumping height by providing a pathway to store more energy under the actuation and structural limits. Although these results are based on a C^0 piecewise linear force-displacement curve, the principles can be directly extended to any C^n $(n \geq 1)$ nonlinear curves.

3.2. TENSION (POSITIVE DISPLACEMENT) SECTION OF THE FORCE-DISPLACEMENT CURVE

In the previous section, we analyzed the effect of utilizing nonlinear properties to increase the energy storage in the compression section (negative displacement) of the force-displacement curve. In order to fully comprehend the effect of nonlinear springs on jumping, we also need to study the tension (positive displacement) section of the force-displacement curve. In this section, we consider three different stiffness profiles (figure 6). The compressive part of these force-displacement curves are same as the one in the previous section with positive $\hat{k}_3$ $(=+0.7)$; while the tension parts of these curves ($\hat{k}_1$) differ. Three different $\hat{k}_1$ values are chosen: $\hat{k}_1 = 1$ represents a spring with the same tension stiffness as the constant linear spring discussed in the previous section. $\hat{k}_1 = 0.5$ and $\hat{k}_1 = 5$ represent springs with softer and stiffer (with respect to $\hat{k}_1 = 1$) tension stiffness, respectively (figure 6).

Figure 7(a) shows the vertical displacement of both of the masses according to the three different tension stiffness coefficients. Based on the results of figure 7(c), we can observe that changing the tension (positive displacement) stiffness of the force-displacement profile does not affect the maximum height that the center of gravity of the mechanism can reach. On the other hand, the stiffness of the tension section has a significant effect on the oscillations of two constituent masses of the mechanism. Based on the results of figure 7(b), we can observe that increasing the tension stiffness will decrease the amplitude of the internal oscillations of the mechanism, but increases their frequency. In the next section, we try to *qualitatively* explain these observations analytically by performing a modal analysis on a simplified system.

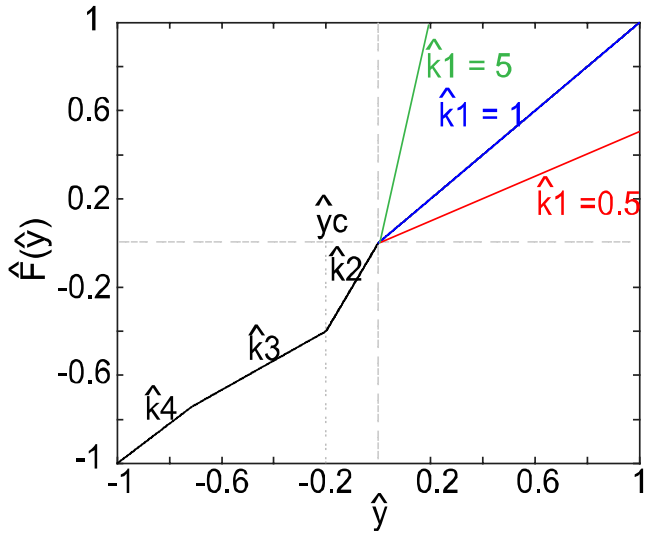

Figure 6. Three different piecewise linear force-displacement curves with the same compression section ($\hat{k}_2 = 2$, $\hat{k}_3 = +0.7$, $\hat{k}_4 = 0.9$, $\hat{y}_c = -0.2$) but different tension stiffness coefficients.

3.2.1. THE EFFECT OF TENSION STIFFNESS ON THE JUMPING MOTION OF THE CENTER OF GRAVITY AND THE INTERNAL OSCCILLATIONS

Figure 1(b) shows the jumping mechanism at its airborne phase. We derived the equations of motion for the case where $m_1 = m_2 = m$ (equation 5). At this section we consider a more general case where the upper and the lower mass can be different. We can show that the motion of the both masses is governed by the following system of equations:

$$\begin{aligned} m_1\ddot{z}_1 &= F(z_2 - z_1) - m_1 g \\ m_2\ddot{z}_2 &= -F(z_2 - z_1) - m_2 g, \end{aligned} \quad (13)$$

where z_2 and z_1 are measured from the free length and the ground, respectively and $F(z_2 - z_1)$ is a nonlinear function. Here, we simply use the tension stiffness k_1 to represent the stiffness characteristics around the equilibrium ($z_2 = 0$). This is a reasonable simplification because the post-jump phase of motion *initially* occurs when the spring is under tension. Therefore, we can simplify the equations of motion in a linear matrix form:

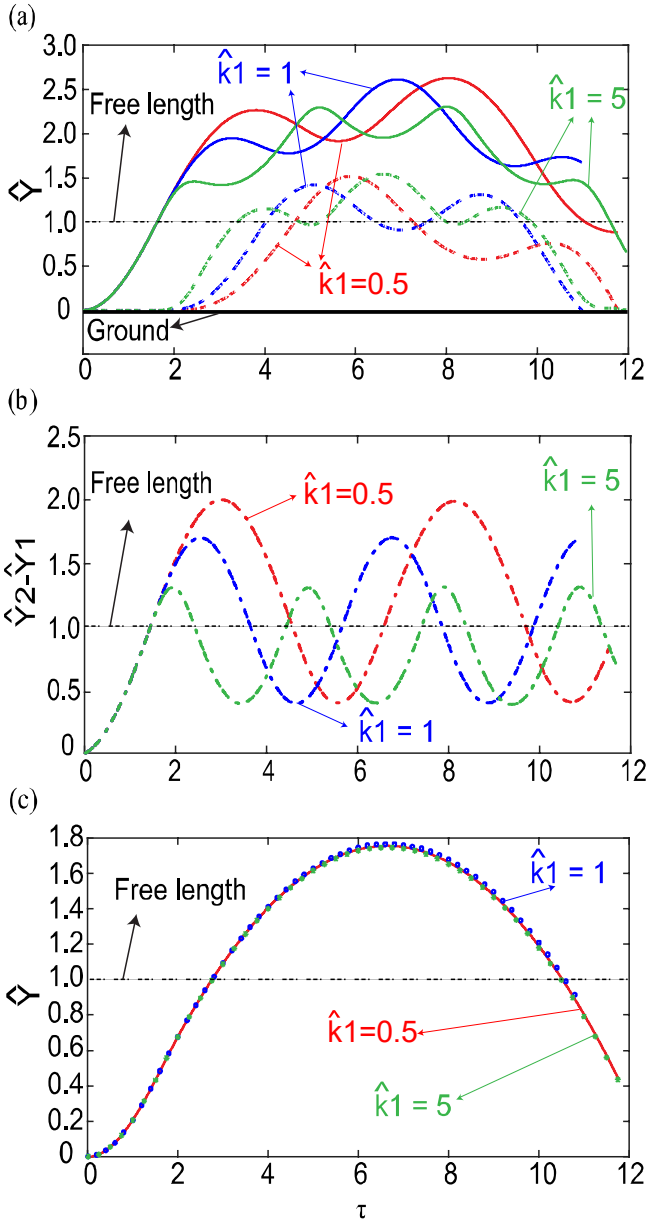

Figure 7. (a) Vertical displacement of the upper mass (solid line) and the lower mass (dashed line). (b) Internal oscillations of the jumping mechanism. (c) Vertical displacement of the center of gravity. Colors are the same as in figure 6.

$$\begin{pmatrix}\ddot{z}_1\\ \ddot{z}_2\end{pmatrix}=\begin{pmatrix}-\frac{k_1}{m_1} & \frac{k_1}{m_1}\\ \frac{k_1}{m_2} & \frac{k_1}{m_2}\end{pmatrix}\begin{pmatrix}z_1\\ z_2\end{pmatrix}+\begin{pmatrix}-g\\ -g\end{pmatrix}\Leftrightarrow \underline{\ddot{Z}}=[K]\underline{Z}-\underline{g}. \tag{14}$$

We can find the eigenvalues and the corresponding eigenvectors of the stiffness matrix ($[K]$) as follows:

$$\lambda_1=0,\underline{v_1}=\begin{pmatrix}1\\ 1\end{pmatrix}$$
$$\lambda_1=-k_1\frac{m_1+m_2}{m_1m_2},\underline{v_2}=\begin{pmatrix}-m_2/m_1\\ 1\end{pmatrix}. \tag{15}$$

One can show that, by diagonalization:

$$[K]=[V][\Lambda][V]^{-1}, \tag{16}$$

where:

$$[V]=\begin{pmatrix}\underline{v_1} & \underline{v_2}\end{pmatrix}=\begin{pmatrix}1 & -\frac{m_2}{m_1}\\ 1 & 1\end{pmatrix},$$
$$[\Lambda]=\begin{pmatrix}\lambda_1 & 0\\ 0 & \lambda_2\end{pmatrix}=\begin{pmatrix}0 & 0\\ 0 & -k_1\frac{m_1+m_2}{m_1m_2}\end{pmatrix}. \tag{17}$$

Therefore, we can update equation 14 as follows:

$$\underline{\ddot{Z}}=[V][\Lambda][V]^{-1}\underline{Z}-\underline{g}. \tag{18}$$

Pre-multiply both sides of equation (18) by V^{-1}:

$$[V]^{-1}\underline{\ddot{Z}}=[\Lambda][V]^{-1}\underline{Z}-[V]^{-1}\underline{g}, \tag{19}$$

and define $\underline{U}=[V]^{-1}\underline{Z}$. That is:

$$\underline{U}=\begin{pmatrix}u_1\\ u_2\end{pmatrix}=[V]^{-1}\underline{Z}=\begin{pmatrix}\frac{m_1z_1+m_2z_2}{m_1+m_2}\\ \frac{m_1}{m_1+m_2}(z_2-z_1)\end{pmatrix}. \tag{20}$$

Based on equation 20, we can observe that u_1 and u_2 represent the position of the center of gravity and the magnitude of the internal oscillatory motion of the mechanism, respectively. Using $\underline{U}$ as the new state variable, we can update equation 18:

$$\underline{\ddot{U}}=[\Lambda]\underline{U}-[V]^{-1}\underline{g}. \tag{21}$$

By substituting $[\Lambda]$ and $[V]^{-1}$ matrices into equation 21, we have:

$$\begin{pmatrix}\ddot{u}_1\\ \ddot{u}_2\end{pmatrix}=\begin{pmatrix}0 & 0\\ 0 & -k_1\dfrac{m_1+m_2}{m_1m_2}\end{pmatrix}\begin{pmatrix}u_1\\ u_2\end{pmatrix}-\begin{pmatrix}\dfrac{m_1}{m_1+m_2} & \dfrac{m_2}{m_1+m_2}\\ -\dfrac{m_1}{m_1+m_2} & \dfrac{m_1}{m_1+m_2}\end{pmatrix}\begin{pmatrix}g\\ g\end{pmatrix}. \quad (22)$$

This means that:

$$\ddot{u}_1=-g\left(\frac{m_1}{m_1+m_2}+\frac{m_2}{m_1+m_2}\right)=-g$$
$$\ddot{u}_2=-k\left(\frac{m_1+m_2}{m_1m_2}\right)u_2. \quad (23)$$

We can clearly see that the acceleration of the center of gravity is independent of the stiffness of the tension section and is always equal to $(-g)$. Therefore, we can conclude that, even with different tension stiffness coefficients, the center of gravity movement of these mechanisms will be the same as long as the initial stored energy based on compression section is the same. We also observed this for the actual nonlinear system (figure 7(c)). We can also derive the frequency of the internal oscillations of the simplified mechanism as follows:

$$\Omega=\sqrt{\frac{m_1+m_2}{m_1m_2}k_1}. \quad (24)$$

Although equation 24 is derived for a simplified mechanism and does not provide the exact frequency of oscillations for the nonlinear system, it suggests that the internal oscillations of the mechanism depend on the tension stiffness, which is in agreement with the numerical simulation results, based on the actual nonlinear system (figure 7(b)).

Therefore, although changing the stiffness coefficient of the tension section does not change the jumping behavior of the center of mass, it has a significant effect on the internal oscillations of the system. Consequently, utilizing a specific tension stiffness for the mechanism is a choice that depends on the desired internal behavior of the mechanism, and may vary in different applications.

4. CONCLUSION AND DISCUSSION

In this study, we investigate the dynamic behaviors of a jumping mechanism consisting two masses connected by a nonlinear spring characterized by a generic piecewise linear function. We derive the non-dimensional equations of motion and solve them numerically to elucidate the effect of two main sections of the nonlinear force-displacement curve, i.e. compression and tension, on the jumping performance of the system. We observe that utilizing nonlinear springs can store more initial strain energy in the system compared to a linear spring, and can lead to higher jumps both in term of the center of gravity and the individual masses. However, the energy efficiency of the jumping would drop slightly. In addition, we saw that the stiffness coefficient of the tension section of the nonlinear force-displacement curve does not affect the airborne motion of the center of gravity. Although it has a significant effect on the internal oscillations of the jumping mechanism after it leaves the ground. Researchers have investigated various approaches for creating nonlinear spring characteristics, from combining different linear springs [34] to fluidic [33,35] and bi-stable [36] origami. Therefore, results of this study is generic and can be applied to a variety of robotic designs to create more efficient and optimized jumping and hopping performance.

ACKNOWLEDGMENTS

S. Sadeghi, B. Betsill and S. Li acknowledge the support by the National Science Foundation (Award # CMMI-1633952 and CMMI-1751449 CAREER) and the startup funding from Clemson University. P. Tallapragada acknowledges the support by the National Science Foundation (Award # CMMI-1563315).

REFERENCES

[1] Raibert, M. H., 1986, *Legged Robots That Balance*, MIT Press.

[2] Aerts, P., 1998, "Vertical Jumping in Galago Senegalensis: The Quest for an Obligate Mechanical Power Amplifier," Philos. Trans. R. Soc. B Biol. Sci., **353**(1375), pp. 1607–1620.

[3] Roberts, T. J., 2003, "Probing the Limits to Muscle-Powered Accelerations: Lessons from Jumping Bullfrogs," J. Exp. Biol., **206**(15), pp. 2567–2580.

[4] Sayyad, A., Seth, B., and Seshu, P., 2007, "Single-Legged Hopping Robotics Research - A Review," Robotica, **25**(5), pp. 587–613.

[5] Bergbreiter, S. E., 2007, "Autonomous Jumping Microrobots," ProQuest Diss. Theses, **3306062**, p. 150.

[6] Raibert, M. H., Brown, H. B., and Chepponis, M., 1984, "Experiments in Balance with a 3D One-Legged Hopping Machine," Int. J. Rob. Res., **3**(2), pp. 75–92.

[7] Zhao, J., Xu, J., Gao, B., Xi, N., Cintron, F. J., Mutka, M. W., and Xiao, L., 2013, "MSU Jumper: A Single-Motor-Actuated Miniature Steerable Jumping Robot," IEEE Trans. Robot., **29**(3), pp. 602–614.

[8] Haldane, D. W., Plecnik, M. M., Yim, J. K., and Fearing, R. S., 2016, "Robotic Vertical Jumping Agility via Series-Elastic Power Modulation," Sci. Robot., **1**(1), p. eaag2048.

[9] Haldane, D. W., Plecnik, M., Yim, J. K., and Fearing, R. S., 2016, "A Power Modulating Leg Mechanism for Monopedal Hopping," IEEE Int. Conf. Intell. Robot. Syst., 2016, pp. 4757–4764.

[10] Koditschek, D. E., and Bühler, M., 1991, "Analysis of a Simplified Hopping Robot," Int. J. Rob. Res., **10**(6), pp. 587–605.
[11] Maier, K. D., 2001, "Neural Network Based Control of Legged Hopping Systems," pp. 115–120.
[12] Schammass, A., Caurin, G. A. P., and Valente, C. M. O., 2001, "Control of a One-Legged Robot with Energy Savings," J. Brazilian Soc. Mech. Sci., **23**(1), pp. 41–48.
[13] Albro, J., and Bobrow, J., 2001, "Optimal Motion Primitives for a 5 Dof Experimental Hopper," Robot. Autom, 2001, pp. 3630–3635.
[14] Matsuoka, K., 1979, "A Model of Repetitive Hopping Movements in Man," Proc. Fifth World Congr. Theory Mach. Mech., pp. 1168–1171.
[15] Raibert, M. H., Chepponis, M., and Brown, H. B., 1986, "Running on Four Legs As Though They Were One," IEEE J. Robot. Autom., **2**(2), pp. 70–82.
[16] Lee, W., and Raibert, M., 1991, "Control of Hoof Rolling in an Articulated Leg," Proceedings. 1991 IEEE Int. Conf. Robot. Autom., pp. 1386–1391.
[17] Kovač, M., Fuchs, M., Guignard, A., Zufferey, J. C., and Floreano, D., 2008, "A Miniature 7g Jumping Robot," Proc. - IEEE Int. Conf. Robot. Autom., pp. 373–378.
[18] Zhang, J., Song, G., Qiao, G., Meng, T., and Sun, H., 2011, "An Indoor Security System with a Jumping Robot as the Surveillance Terminal," IEEE Trans. Consum. Electron., **57**(4), pp. 1774–1781.
[19] Dupuis, E., Montminy, S., Farhat, M., and Champliaud, H., 2006, "Mechanical Design of a Hopper Robot for Planetary," (1), pp. 1–8.
[20] Scarfogliero, U., Stefanini, C., and Dario, P., 2009, "The Use of Compliant Joints and Elastic Energy Storage in Bio-Inspired Legged Robots," Mech. Mach. Theory, **44**(3), pp. 580–590.
[21] Zhao, J., Xi, N., Gao, B., Mutka, M. W., and Xiao, L., 2010, "Design and Testing of a Controllable Miniature Jumping Robot," IEEE/RSJ 2010 Int. Conf. Intell. Robot. Syst. IROS 2010 - Conf. Proc., pp. 3346–3351.
[22] Tsukagoshi, H., Sasaki, M., Kitagawa, A., and Tanaka, T., 2005, "Design of a Higher Jumping Rescue Robot with the Optimized Pneumatic Drive," Proc. - IEEE Int. Conf. Robot. Autom., **2005**(April), pp. 1276–1283.
[23] Kim, D. H., Lee, J. H., Kim, I., Noh, S. H., and Oho, S. K., 2008, "Mechanism, Control, and Visual Management of a Jumping Robot," Mechatronics, **18**(10), pp. 591–600.
[24] Kesner, S., Plante, J., Dubowsky, S., and Boston, P., 2007, "A Hopping Mobility Concept for a Rough Terrain Search and Rescue Robot," Adv. Climbing Walk. Robot. Proc., pp. 271–280.
[25] Dubowsky, S., Kesner, S., Plante, J., and Boston, P., 2008, "Hopping Mobility Concept for Search and Rescue Robots," Ind. Robot An Int. J., **35**(3), pp. 238–245.
[26] Armour, R., Paskins, K., Bowyer, A., Vincent, J., and Megill, W., 2007, "Jumping Robots: A Biomimetic Solution to Locomotion across Rough Terrain," Bioinspiration and Biomimetics, **2**(3).
[27] Yamada, A., Watari, M., Mochiyama, H., and Fujimoto, H., 2008, "An Asymmetric Robotic Catapult Based on the Closed Elastica for Jumping Robot," pp. 232–237.
[28] Yamada, A., Mameda, H., Mochiyama, H., and Fujimoto, H., 2010, "A Compact Jumping Robot Utilizing Snap-through Buckling with Bend and Twist," IEEE/RSJ 2010 Int. Conf. Intell. Robot. Syst. IROS 2010 - Conf. Proc., pp. 389–394.
[29] M'Closkey, R. T., and Burdick, J. W., 1993, "Periodic Motions of a Hopping Robot With Vertical and Forward Motion," Int. J. Rob. Res., **12**(3), pp. 197–218.
[30] Fiorini, P., and Burdick, J., 2003, "The Development of Hopping Capabilities for Small Robots," Auton. Robots, **14**(2–3), pp. 239–254.
[31] Lee, C. M., Goverdovskiy, V. N., and Temnikov, A. I., 2007, "Design of Springs With 'negative' stiffness to Improve Vehicle Driver Vibration Isolation," J. Sound Vib., **302**(4–5), pp. 865–874.
[32] Wang, Y., Li, S., Neild, S. A., and Jiang, J. Z., 2017, "Comparison of the Dynamic Performance of Nonlinear One and Two Degree-of-Freedom Vibration Isolators with Quasi-Zero Stiffness," Nonlinear Dyn., **88**(1), pp. 635–654.
[33] Sadeghi, S., and Li, S., 2017, "Harnessing the Quasi-Zero Stiffness From Fluidic Origami for Low Frequency Vibration Isolation," *Volume 2: Modeling, Simulation and Control of Adaptive Systems; Integrated System Design and Implementation; Structural Health Monitoring*, ASME, p. V002T03A008.
[34] Kovacic, I., Brennan, M. J., and Waters, T. P., 2008, "A Study of a Nonlinear Vibration Isolator with a Quasi-Zero Stiffness Characteristic," J. Sound Vib., **315**(3), pp. 700–711.
[35] Li, S., Fang, H., and Wang, K. W., 2016, "Recoverable and Programmable Collapse from Folding Pressurized Origami Cellular Solids," Phys. Rev. Lett., **117**(11), pp. 1–5.
[36] Fang, H., Li, S., Ji, H., and Wang, K. W., 2017, "Dynamics of a Bistable Miura-Origami Structure," Phys. Rev. E, **95**(5), p. 52211.